

Perspectives

Aerosol dynamics and the synthesis of fine solid particles

Rajdip Bandyopadhyaya¹, Anshuman A. Lall, Sheldon K. Friedlander*

Department of Chemical Engineering, University of California at Los Angeles, Los Angeles, CA 90095, USA

Received 10 August 2003; accepted 13 October 2003

Abstract

Aerosol dynamics (AD) is the discipline that deals with changes in particle size distributions in space and time. AD is based on (1) certain fundamental principles embodied in a set of equations, (2) experimental methods and instrumentation and (3) numerical and computational methods. Over the last few decades, AD has emerged as an enabling discipline in the design of aerosol reactors employed in the gas phase synthesis of fine powders, the characterization of particle emissions from sources such as coal-fired power plants and the atmospheric aerosol. The development of basic AD concepts since early in the 20th century is traced to the present. Major gaps that remain in the field and likely advances over the next few years are discussed. Although accurate predictions of particle size from first principles are difficult to make in practical applications, AD principles can be used to explain trends in product properties for flame and laser ablation reactors that operate under very different temperatures and quench rates.

© 2004 Elsevier B.V. All rights reserved.

Keywords: Aerosol Dynamics; Flame reactor; Laser ablation; Nanoparticle size; Aerosol Reactors; Collision–coalescence

1. What is aerosol dynamics?

Small solid particles form in high temperature gases when vapors of substances with very low volatility are cooled. This phenomenon is exploited in the manufacture of nanoparticles for use as reinforcing fillers [1,2], catalysts [3], sensor coatings [4,5] and in the fabrication of optical fibers [6]. Certain technologies generate fine solid particles unintentionally. Examples range from welding fumes [7] and solid fuel rocket emissions to large scale industrial installations that include coal-fired power plants [8,9] and metallurgical operations such as the smelting of ores. Emissions from these sources may cause health and other environmental problems. Finally, natural phenomena such as the volatilization of meteoritic bodies that enter earth's atmosphere may produce vapors that condense to form fine solid particles.

The principles that describe particle formation and properties in many of these systems fall within the domain of *aerosol dynamics*. Aerosol dynamics (AD) can be

defined as the study of the factors that determine the distribution of aerosol properties with respect to particle size and other morphological parameters such as surface area and fractal dimension; these distributions change with position and time in both industrial and natural processes [10]. Distributed aerosol properties include (but are not limited to) the number, mass, surface area and light scattering. AD is a discipline based on (1) certain fundamental principles embodied in a set of equations, (2) experimental methods and instrumentation, and (3) numerical and computational methods. AD is playing an increasing role in the commercial synthesis of fine powdered materials. (See the comprehensive book by Kodas and Hampden-Smith [11] and the excellent review on flame reactors by Stark and Pratsinis [3] that appeared in this journal).

In this perspective, we trace the development of the fundamental principles of AD from their inception, almost a century ago, to the present. This leads to a discussion of likely future developments over the next few years. We review the reasons why serious limitations remain on our ability to predict product properties. Although we often cannot make detailed predictions, we give an example of how basic concepts can be used to explain *trends* in particle size for two types of aerosol reactors, namely flame and laser ablation reactors.

* Corresponding author. Fax: +1-310-206-4107.

E-mail address: skf@ucla.edu (S.K. Friedlander).

¹ Present address: Chemical Engineering Department, Indian Institute of Technology, Kanpur 208016, India.

2. Terminology

Some of the most important fine particle commercial products, including reinforcing fillers, catalysts and sensor coatings fall in the size range smaller than 100 nm. In the rest of the paper, we limit consideration to particles in this size range, often referred to as *nanoparticles*. Nanoparticle products can be characterized using the following terms based on their morphological properties:

- Primary particles, the smallest identifiable individual particles, are usually in the size range between 5 and 50 nm. These are often present as individual crystals.
- Aggregates are assemblies of primary particles held together by strong bonds, probably ionic/covalent in nature.
- Agglomerates are assemblies of aggregates held together by weak bonds which may be due to van der Waals forces or ionic/covalent bonds operating over very small contact areas. Agglomerates may break up to form aggregates, for example, when they are blended with polymers in the manufacture of rubber.

This terminology is used by manufacturers of inorganic oxide aerosol products and carbon black. It may also be helpful for describing aerosol emissions in the size range smaller than 100 nm from diesel engines and other sources of incomplete combustion. However this terminology is not adequate for the *quantitative* characterization of aggregate/agglomerate structures, including the bond energies that hold primary particles in aggregate chains together, which are important in many applications. This point is addressed later in the paper.

3. An AD chronology

The origin of aerosol dynamics can be traced to the beginning of the last century. A very early contribution was due to Smoluchowski [12] who derived an expression for the collision frequency of spherical particles in Brownian motion. In the Smoluchowski theory, the particle collision rate is assumed to be a diffusion limited process, and collision is followed by instantaneous coalescence. The principal application at the time was to suspensions of colloidal particles in liquids. Whytlaw-Gray and Patterson [13] showed that the Smoluchowski theory was in fair agreement with their experimental measurements of the coagulation of aerosols composed of various materials, many of them nonspherical solid particles, often in the form of aggregates. Subsequently, Fuchs [14] extended Smoluchowski's theory to particle sizes smaller than the mean free path of the carrier gas, which is about 60 nm for air at 298 K and one atmosphere. Nanoparticles therefore come under this free molecular size regime.

Prior to particle formation in a high temperature gas, the supersaturated state may result from physical processes or chemical reactions. In the early stages of formation, particle concentrations are very high so that collision frequencies are also very high. Lai et al. [15] showed that size distributions approach an asymptotic form, independent of the initial size distribution, for certain important collision frequency functions. This has important practical implications: The details of the initial distributions of very small aerosols are often difficult to determine experimentally or theoretically. However, after a few particle collision times, the initial properties have little effect on the *normalized* size distribution. Quantitative calculations of the time to reach the asymptotic form for different initial distributions were given by Hidy and Lilly [16] and Vemury and Pratsinis [17]. Numerical methods of calculating size distributions can therefore be checked by comparing calculated distributions with the known asymptotic forms.

A major breakthrough in the way the field of aerosol dynamics was viewed came in the early 1970's when Whitby et al. [18] showed that with a combination of an electrical mobility analyzer (developed in his laboratory) and an optical particle counter, they could measure the particle size distribution of the atmospheric aerosol in a few minutes. The size range covered was from about 10 nm to 5 μm . This capability changed the way researchers viewed the field of aerosol dynamics. For the first time, we were able to follow changes in the size distribution on an almost real time basis. These measurement systems were soon applied not only to the atmospheric aerosol but also to aerosol emissions from industrial installations and vehicular sources. However, it is still not possible to measure size distributions on-line in industrial aerosol reactors producing commercial powders because of their high concentrations, temperatures and, often, corrosive operating conditions.

Until the 1970's, AD theory was limited by the Smoluchowski assumption that all particle collisions result in instantaneous coalescence. This assumption clearly did not apply to commercially produced powders such as nanoparticle silica. To explain silica particle formation, Ulrich and Subramanian [19] introduced the concept of the characteristic time for coalescence or sintering. They calculated this for silica from the Frenkel theory, which gave the time taken for a nearly spherical liquid droplet to relax to the spherical form by viscous flow. They assumed that the amorphous silica particles behaved like highly viscous liquid droplets. The analysis went even further: They assumed that there is a class of particle formation processes in which (1) the chemical reactions that lead to particle formation are so fast that the particle cloud forms practically instantaneously and (2) the material vapor pressure is so low that nucleation is practically instantaneous producing an aerosol of very high initial concentration, which then coagulates. Particle growth thus could be modeled by a collision-coalescence mechanism and the final primary particle size was not affected by rates of chemical reaction and nucleation.

Following Ulrich's introduction of a coalescence time, Koch and Friedlander [20] showed that the equations of aerosol dynamics (based on Smoluchowski theory) for aerosol size distributions could be extended to incorporate the rate of coalescence in addition to the collision frequency. For this purpose, the size distribution function was generalized to include both particle volume and surface area as independent variables. They found that the dynamic equations depended on two characteristic times, one for collision and the other for coalescence. Later, Windeler et al. [21] suggested that the primary particle size could be estimated by equating the collision and coalescence times. An explanation for why this criterion holds based on the equations of AD was given later by Friedlander [10]. The criterion is used later in this paper in a discussion of the comparative behavior of flame and laser ablation reactors.

In 1979, Forrest and Witten [22] calculated density–density correlation functions for the spatial distribution of particles in aggregates from electron micrographs of fumed silica aggregates obtained from the Cabot, and their own data for aggregates of iron and zinc nanoparticles. They found that a power law relationship frequently could describe the fall-off in density of the particles as a function of distance from a given particle. Values of the power law exponent could be calculated for various particle collision mechanisms and varied depending on the collision algorithm. The power law exponent could be related to the *fractal dimension*. Tandon and Rosner [23] generalized the equations of aerosol dynamics to include aggregate structure by incorporating the fractal dimension among the independent variables used to characterize the generalized size distribution function.

Schmidt-Ott [24] showed that chain aggregates of particles were not rigid structures. When heated, their structure became more compact. Subsequently, Friedlander et al. [25] and Suh and Friedlander [26] discovered that individual nanoparticle chain aggregates (NCA) made of primary particles (of nanometric dimension) may display elastic behavior. Under tension, aggregates straighten and lengthen until they become taut. Eventually, they break and then contract. This phenomenon may help explain why reinforcing fillers such as carbon black and fumed silica have such large effects on the elastic properties of commercial rubber, composed of NCA fillers blended with polymers.

To estimate coalescence times for nanoparticles in contact, the practice has been to use models developed for micron sized and larger particles of the type used in ceramic powder sintering. The models, derived for liquid or solid particles, are based on bulk properties for viscosity, surface tension and solid state diffusion coefficients. Such models are likely to break down for nanoparticles, because a large fraction of the molecules that compose the particles are near the particle surface; bulk properties may no longer adequately describe the coalescence process. Based on a suitable interatomic potential, Zachariah and Carrier [27] made molecular dynamics (MD) calculations of the time

required for the coalescence of silicon nanoparticles. The calculations do not require use of the bulk properties that appear in macroscopic sintering theories.

4. Future developments in AD

Despite significant advances, it is still not possible to predict accurately the properties of fine solid particles generated from hot vapors of materials with very low vapor pressure. This limitation is encountered in technological systems such as aerosol reactors and emissions from installations such as coal-fired power plants and smelters. Why is this so? One reason has been the uncertainty concerning nanoscale coalescence processes discussed above, and its effects on aggregate structure and mechanical properties. Various molecular simulation techniques like MD, Monte Carlo and other ab-initio methods are likely to become increasingly important in efforts to improve our understanding of nanoscale AD. At first, these can be used in making improved predictions of primary particle size. To test the theory, there is a need for novel laboratory aerosol reactors with well-defined geometry and fluid mechanics [28].

It is likely that MD will also prove useful in estimating the contact area between primary particles when there is partial coalescence, and consequently the bond energies that hold particles in chain aggregates together. This is not considered in existing MD calculations. An important application is in the prediction of the properties of composites of NCA blended with polymers such as rubber. Other applications are to the break up of aggregates resulting from impaction and shear. To test theoretical predictions, we will need to measure properties like tensile strength and elastic modulus of *individual* chain aggregates using novel techniques as well as existing methods such as atomic force microscopy.

Experimental data for metal oxide nanoparticles indicate that they are often crystalline [29]; crystal structure significantly affects particle properties including catalytic effects. MD calculations should help in estimating the time required for amorphous particles to crystallize and the crystal structure that they reach.

Much effort will be needed to import the results of molecular simulations into predictions of the size distributions of primary particles and their aggregates. It is likely that this will begin with the AD equations, based on Smoluchowski theory, but the classical mean field theory may be replaced eventually by multiscale methods. These methods combine various sub models for the overall dynamic system, in order to describe events over different length and time scales [30]. For the present case, collisions among primary particles and with aggregates can be handled by Brownian Dynamics simulation [31]. Coupled to this, at a smaller length scale, the complete or partial coalescence of individual primary particles within an aggregate can be computed using MD.

Another limitation on our ability to predict accurately the properties of particulate products, noted by Stark and Pratsinis [3], is the difficulty in incorporating AD in the relevant fluid dynamic, heat and mass transfer regimes, except for simple geometries such as tubular reactors used in the manufacture of optical fibers. This difficulty is compounded by the strong dependence of the coalescence rate on the local gas temperature. Despite these limitations, AD concepts are proving to be useful in design. In the next sections, we give an example of an application to the explanation of trends in experimental data on particle size.

Finally, the condensation of multicomponent vapors leads to fine particle formation. This results in an ultrafine particle mode in emissions from coal combustion [8,9]. The particle phase components may be immiscible or only partially miscible [32]. Coalescence rates when such particles are in contact will be hard to estimate. Condensation from multicomponent vapors merits further experimental and theoretical investigation.

5. Experimental data on particle size trends for two reactor types

Although we often cannot use AD for accurate prediction of product properties, it can be helpful in analyzing trends. With this objective, we examine two sets of particle size data from two different types of laboratory reactors, but for similar sets of aerosol materials. Windeler et al. [21,33] and Ullmann et al. [34] reported results for the synthesis of nanoparticles by flame and laser ablation processes, respectively. In the studies of Windeler et al., precursor vapors (of volatile metal compounds of niobium, titanium, aluminium) mixed with nitrogen were fed into a methane-air flame [33]. The precursor vapor concentrations were set to produce the same aerosol volumetric concentrations for each material. A flame temperature near 2000 K

Table 1

Experimental data on primary particle size of different oxides generated in flame reactor [33] and by laser ablation [34]

Aerosol material	Geometric mean particle diameter (nm) (Flame reactor) ^a	Modal particle diameter (nm) (Laser ablation) ^b
Niobia (Nb ₂ O ₅)	21.6	13
Titania (TiO ₂)	11.1	5.9
Alumina (Al ₂ O ₃)	4.1	5.5
Silica (SiO ₂)	–	5.2
Iron oxide (Fe ₂ O ₃)	–	8
Tungsten oxide (WO ₃)	–	8

^a Exit aerosol volumetric concentration $\phi = 3.2 \times 10^{-7}$ for all three oxides.

^b Exit aerosol volumetric concentration ranges from $\phi = 4 \times 10^{-9}$ to 3×10^{-10} for different oxides.

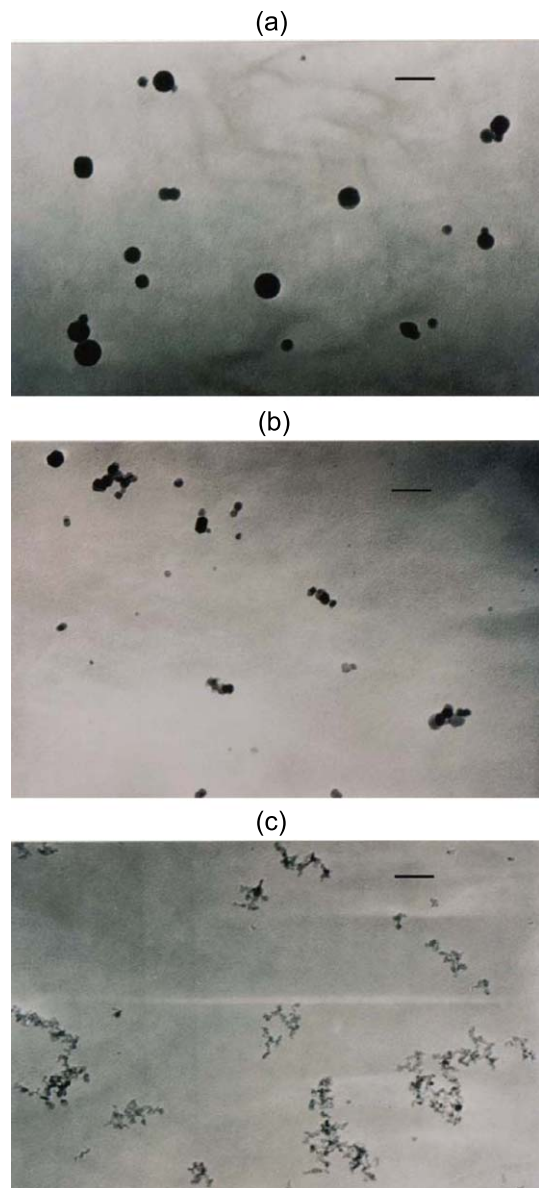


Fig. 1. Transmission electron micrographs of particles of different metal oxides generated in the flame reactor [33], under identical process conditions; (a) niobia, (b) titania, (c) alumina. Scale bar is 50 nm.

caused the precursor to decompose and react with oxygen leading to metal oxide vapors and the formation of oxide nanoparticles.

In later studies by Ullmann et al. [34], a laser beam of a given wavelength was focused on a rotating target consisting of a metal foil. This resulted in ablation of the metal target to form a metal vapor that was oxidized by an oxygen stream to synthesize metal oxide particles. Estimates of temperature in the plume coming off the target are of the order of 20000 K [34]. The aerosol volumetric concentrations for the different metal oxides were nearly equal. However, little is known about the mechanism of particle formation by reactive laser ablation [11]; for the purpose of this analysis, we assume that the collision-

coalescence mechanism is controlling, as in the case of the flame reactor.

Data on primary particle size for different materials, taken from these references are shown in Table 1, with the aerosol volumetric concentration (ϕ) at the exit, in each reactor. To our knowledge, these are the only data for similar sets of data under similar operating conditions in each of the reactors. Data on some of the metal oxides—namely niobia, titania and alumina—are common to both measurement sets. Among these three, niobia and alumina form the largest and smallest primary particles respectively. Table 1 shows that the ratio of maximum to minimum size for the three materials is significantly higher for the flame reactor, compared to laser ablation. In fact in laser ablation, except for niobia, the particle size of the other five oxides falls within the narrow range of 5–8 nm. Therefore in laser ablation, the size is much less dependent on the material involved.

Fig. 1a–c shows transmission electron micrographs of niobia, titania and alumina aerosols made in the flame reactor, data for which are given in Table 1. Niobia forms isolated spherical particles, whereas titania and alumina have progressively smaller primary particles and increasingly more aggregation.

6. Application of AD to the two data bases

A major difference between the two reactors is the temperature at which the metallic oxides form. We hypothesize that the maximum temperature (T_o) and the quench rate (κ) are controlling parameters, and test the hypothesis by evaluating trends in particle size for different materials as a function of κ for the two different T_o . In the analysis of the data, we make the following assumptions:

1. The primary particle size is set by equating the collision and coalescence times [10,21]. This is approximately when growth of the primary particle by coalescence ceases. Later collisions lead to incomplete coalescence, hence neck formation, rather than primary particle growth.
2. The gas containing the particles cools at a constant quench rate for both reactors. This was approximately the case for the cooling portion of the flow in the flame reactor [33].
3. Mixing of the particle containing gases with the room temperature carrier gas tends to reduce ϕ along the reactor. On the other hand, the decreasing gas temperature tends to increase ϕ . In consideration of these two opposing effects, we have used a constant value of ϕ , the measured exit value, to calculate the characteristic collision time. In addition, the collision time is essentially independent of material properties and is only a weak function of temperature [10].
4. The characteristic coalescence time, on the other hand, depends strongly on material properties (especially the solid state diffusivity) and temperature [10]. Coalescence times based on literature values of bulk solid state

diffusion coefficients were calculated for the three substances [21], since diffusion rates for other mechanisms (such as surface and grain boundary diffusion [10]) are not available.

Finally, we emphasize that, in the results that follow, we study trends in particle size and do not seek to predict its absolute value.

Fig. 2 shows the characteristic collision and coalescence times as a function of the temperature of a flame reactor, operated at: $T_o = 2000$ K, $\kappa = 10^5$ K s $^{-1}$ and $\phi = 10^{-7}$. Since the coalescence time is strongly material dependent, it is plotted separately for alumina, titania and niobia. However, the collision time appears as a single curve, as it is nearly material independent and all the oxides were synthesized with same ϕ . As an illustrative example, consider the coalescence curve of alumina and the collision curve. At short times in the reactor (before the two curves intersect in Fig. 2), all collisions lead to complete coalescence, since the time required for coalescence is smaller. Particle size continues to increase with each collision, until the time of intersection. From this point onwards, coalescence slows because of the sharp decrease of solid state diffusivity with temperature. As a result, partial coalescence would generate aggregates, connected by necks between primary particles. This is seen in the micrographs of alumina aggregates shown in Fig. 1c. Incomplete coalescence also leads to small primary particles for alumina, as found experimentally. Niobia, with a much higher solid state diffusivity at a given temperature, has coalescence times that are orders of magnitude smaller. So in this case, all collisions lead to complete coalescence, and niobia forms relatively large, spherical nanoparticles with no aggregates (Fig. 1a). Finally, with an intermediate value of diffusivity, titania forms small aggregates, with particle size in between that of alumina and niobia (Fig. 1b).

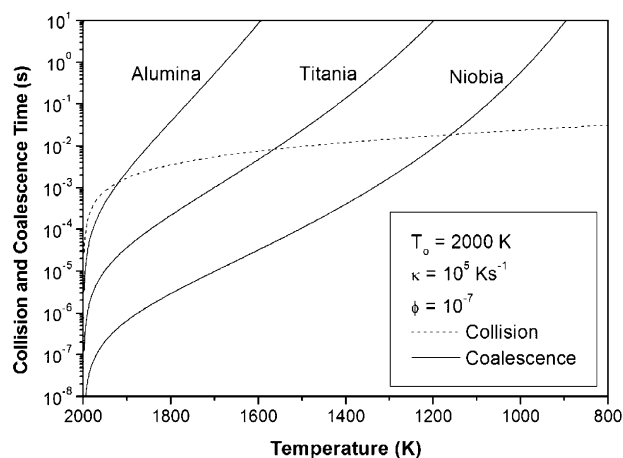


Fig. 2. Variation of characteristic collision and coalescence time for different aerosol material, as a function of temperature, in a typical operation of a flame reactor.

Fig. 3 shows calculated final primary particle sizes for the three oxides as a function of κ with $T_o = 2000$ K and $\phi = 10^{-7}$, corresponding to flame reactor conditions. For a given value of κ , particle sizes for the various oxides differ significantly, especially at lower quench rates. This clearly shows the effect of material properties on particle size. Also the trend is a decrease in size from niobia to alumina, as observed in experiments (Table 1). From the experimental data of Windeler et al. [33], we estimate that quench rates for the flame reactor range from 5×10^4 K s $^{-1}$ to 5×10^5 K s $^{-1}$. This gives us a typical operating regime of flame reactors based on the curves in Fig. 2.

Similar calculations for the same metal oxides were made for $T_o = 20000$ K and $\phi = 10^{-9}$, which corresponds to the laser ablation reactor. As shown in Fig. 4, the particle size obtained is nearly the same for the three oxides. As the quench rate decreases, there is only a small variation in the spread of particle size. This illustrates the material independence of particle size in laser ablation.

In the calculations for the laser ablation reactor (Fig. 4), we have extrapolated the experimental data for solid state diffusivity up to temperatures of 20000 K, far beyond physically realizable solid state behavior. This was done to compare with the results of the flame reactor in Fig. 3, which are based on the same diffusivity data. For purposes of comparison, we have made further calculations starting from different initial temperatures: $T_o = 10000$ and 5000 K, with $\phi = 10^{-9}$. The results show that the particle size is still nearly material independent at these starting temperatures. When T_o is increased from 5000 to 20000 K, the curves in Fig. 4 approach each other and become almost indistinguishable at $T_o = 20000$ K. Therefore, although there is uncertainty about the proper maximum temperature for the laser reactor, the results support our main conclusion that particle size becomes material independent at higher temperatures.

We have also made calculations using a variable ϕ within each of the reactors, with results qualitatively similar to

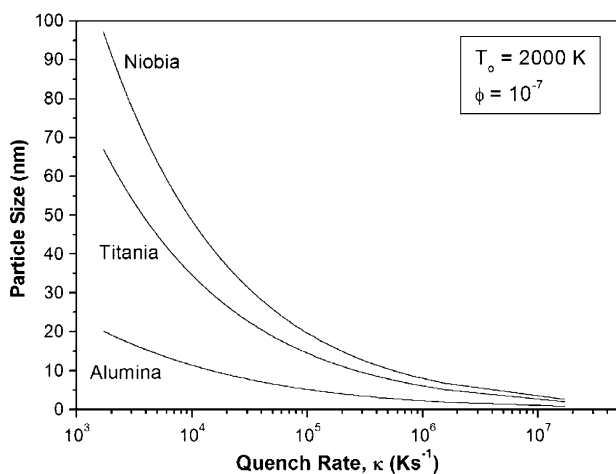


Fig. 3. Variation of primary particle diameter for different aerosol products, as a function of quench rate, for flame reactor conditions.

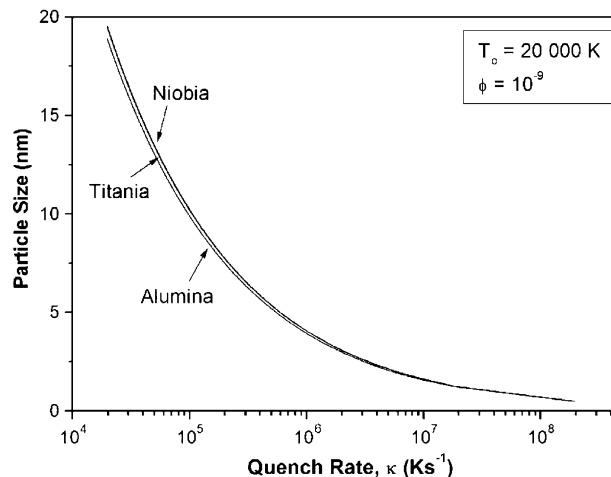


Fig. 4. Variation of primary particle diameter for different aerosol products, as a function of quench rate, under conditions similar to a laser ablation reactor.

those shown in Figs. 3 and 4. Finally, we checked that different order of magnitude values of ϕ in the two reactors (10^{-7} in Fig. 3 and 10^{-9} in Fig. 4) were not the reason for their different behavior. This was done by making a calculation at $T_o = 20000$ K and $\phi = 10^{-7}$, which also gave material independence of particle size at this high temperature. The results of these calculations therefore support the original hypothesis that the maximum temperature and quench rate are major characterizing parameters for the two reactor types.

7. Concluding remarks

Significant advances in AD may be possible through the use of molecular simulations to estimate rates of particle coalescence instead of current practice based on bulk material properties. MD calculations, for example, are likely to work best for particles smaller than about 10 nm and would permit more accurate predictions of primary particle size and crystal structure. Theoretical predictions will need to be tested in well-controlled laboratory reactors. It may also be possible to make MD calculations of the tensile strength, locus of fracture and elastic moduli of nanoparticle chain aggregates. In parallel, there is a need to *measure these properties for individual chain aggregates*. Such information should be of value in developing improved nanocomposite materials and in the control of product quality for aerosol reactors.

Uncertainties in basic aerosol processes and the complex flow and transport regimes in aerosol reactors preclude accurate ab initio predictions of primary particle size and morphology of the aggregate products. However it is possible to use AD concepts to analyze and explain the difference in behavior of laboratory flame and laser ablation reactors producing fine solid particles of the same materials. Thus, in a flame reactor, lower temperature and slower

quenching combines to strongly affect particle size and extent of aggregation, as a function of material properties. On the other hand, in laser ablation, higher operating temperature and quench rate make the particle size almost independent of material properties. These two reactor types therefore represent two limiting behavior patterns based on the time-temperature history in an aerosol reactor. The present analysis is based on some assumptions and we hope that other investigators will test the basic AD concepts on which they are based.

Acknowledgements

The authors wish to acknowledge support through NSF grants CTS 9911133 and CTS 9527999.

References

- [1] A.I. Medalia, G. Kraus, in: J.E. Mark, B. Erman, F.R. Eirich (Eds.), *Science and Technology of Rubber*, Academic Press, New York, 1994, pp. 387–418.
- [2] A.R. Payne, in: G. Kraus (Ed.), *Reinforcement of Elastomers*, Wiley, New York, 1965, pp. 69–123.
- [3] W.J. Stark, S.E. Pratsinis, *Powder Technol.* 126 (2002) 103.
- [4] G. Williams, G.S.V. Coles, *J. Mater. Chem.* 8 (1998) 1657.
- [5] M.K. Kennedy, F.E. Kruis, H. Fissan, B.R. Mehta, S. Stappert, G. Dumpich, *J. Appl. Phys.* 93 (2003) 551.
- [6] S.R. Nagel, J.B. MacChesney, K.L. Walker, in: T. Li (Ed.), *Optical Fiber Communications*, Academic Press, New York, 1985, pp. 11–64.
- [7] B. Rudell, K.R. Akselsson, M.H. Berlin, *J. Aerosol Sci.* 19 (1988) 1153.
- [8] R.C. Flagan, S.K. Friedlander, in: D.T. Shaw (Ed.), *Recent Developments in Aerosol Science*, Wiley, New York, 1978, pp. 25–59.
- [9] R.J. Quann, M. Neville, M. Janghorbani, C.A. Mims, A.F. Sarofim, *Environ. Sci. Technol.* 16 (1982) 776.
- [10] S.K. Friedlander, *Smoke, Dust, Haze*, Oxford Univ. Press, New York, 2000.
- [11] T.T. Kodas, M. Hampden-Smith, *Aerosol Processing of Materials*, Wiley-VCH, New York, 1999.
- [12] M.V. Smoluchowski, *Phys. Z.* 17 (1916) 557.
- [13] R. Whytlaw-Gray, H.S. Patterson, *Smoke: A Study of Aerial Disperse Systems*, Edward Arnold & Co., London, 1932.
- [14] N.A. Fuchs, *The Mechanics of Aerosols*, Dover Publications, New York, 1989.
- [15] F.S. Lai, S.K. Friedlander, J. Pich, G.M. Hidy, *J. Colloid Interface Sci.* 39 (1972) 395.
- [16] G.M. Hidy, D.K. Lilly, *J. Colloid Sci.* 20 (1965) 867.
- [17] S. Vemury, S.E. Pratsinis, *J. Aerosol Sci.* 26 (1995) 175.
- [18] K.T. Whitby, R.B. Husar, B.Y.H. Liu, in: G.M. Hidy (Ed.), *Aerosols and Atmospheric Chemistry*, Academic Press, New York, 1972, pp. 237–264.
- [19] G.D. Ulrich, N.S. Subramanian, *Combust. Sci. Technol.* 17 (1977) 119.
- [20] W. Koch, S.K. Friedlander, *J. Colloid Interface Sci.* 140 (1990) 419.
- [21] R.S. Windeler, K.E.J. Lehtinen, S.K. Friedlander, *Aerosol Sci. Technol.* 27 (1997) 191.
- [22] S.R. Forrest, T.A. Witten, *J. Phys. A: Math. Gen.* 12 (1979) L109.
- [23] P. Tandon, D.E. Rosner, *J. Colloid Interface Sci.* 213 (1999) 273.
- [24] A. Schmidt-Ott, *J. Aerosol Sci.* 19 (1988) 553.
- [25] S.K. Friedlander, H.D. Jang, K.H. Ryu, *Appl. Phys. Lett.* 72 (1998) 173.
- [26] Y.J. Suh, S.K. Friedlander, *J. Appl. Phys.* 93 (2003) 3515.
- [27] M.R. Zachariah, M.J. Carrier, *J. Aerosol Sci.* 30 (1999) 1139.
- [28] K.Y. Park, M. Ullmann, Y.J. Suh, S.K. Friedlander, *J. Nanopart. Res.* 3 (2001) 309.
- [29] W.R. Cannon, S.C. Danforth, J.H. Flint, J.S. Haggerty, R.A. Marra, *J. Am. Ceram. Soc.* 65 (1982) 324.
- [30] S.C. Glotzer, W. Paul, *Annu. Rev. Mater. Res.* 32 (2002) 401.
- [31] G.W. Mulholland, R.J. Samson, R.D. Mountain, M.H. Ernst, *Energy Fuels* 2 (1988) 481.
- [32] S.H. Ehrman, S.K. Friedlander, M.R. Zachariah, *J. Aerosol Sci.* 29 (1998) 687.
- [33] R.S. Windeler, S.K. Friedlander, K.E.J. Lehtinen, *Aerosol Sci. Technol.* 27 (1997) 174.
- [34] M. Ullmann, S.K. Friedlander, A. Schmidt-Ott, *J. Nanopart. Res.* 4 (2002) 499.